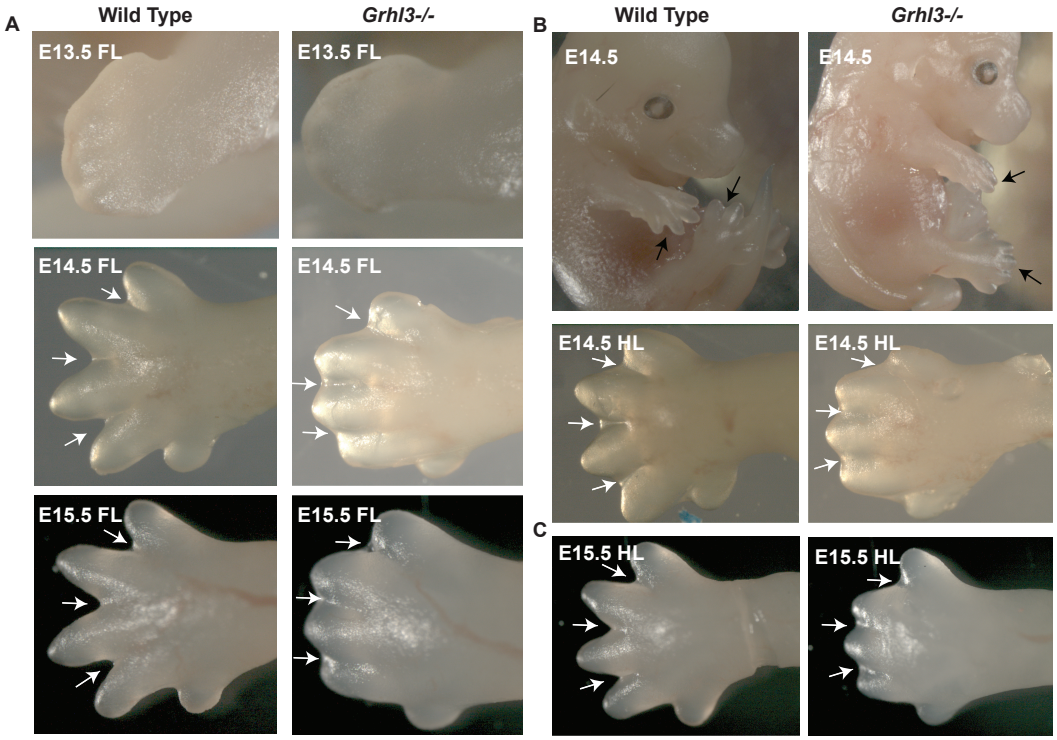

Figure S1. Related to Figure 1. Syndactyly in *Grhl3*$^{-/-}$ embryos is not caused by impaired interdigital cell death
(A) Macroscopic images collected via dissecting scope at several developmental stages. Arrows indicate the interdigital zone. (B) *Grhl3*$^{-/-}$ and littermate WT embryos at E14.5. Arrows point to the forelimbs and hindlimbs. (C) Macroscopic images of WT and *Grhl3*$^{-/-}$ hindlimbs collected via dissecting scope at several E14.5 and E15.5. Arrows indicate the interdigital zone.

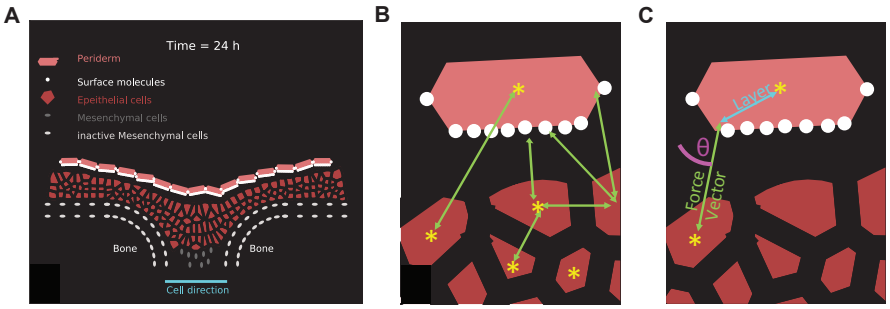

Figure S2. Related to Figure 4 Mathematical modeling suggests that directed cell migration plays a role in the formation of the IET

(A-C) Schematic of the computational model. (A) Model of digit separation. Each cell is represented by a point. The mesenchymal cells (white ellipsoids) lining the bones are inactive and do not migrate. The central mesenchymal cells (grey ellipsoids) migrate towards the bottom center between the two digits. The cell membranes of the epithelial cells (red hexagons) are computed using a Voronoi tessellation of the point cloud and do also migrate. The peridermal cells (pink) have adhesive surface molecules (white dots) on their apical surface and also migrate. (B) The bio-mechanical forces (green arrows) in the tissue are modeled as generalized Morse potentials between the nodes (yellow stars) representing cells. (C) The periderm cells are modeled as rigid elongated hexagons and the sum of the forces acting on the cell center and the surface nodes lead to a translation and rotation of the cells.

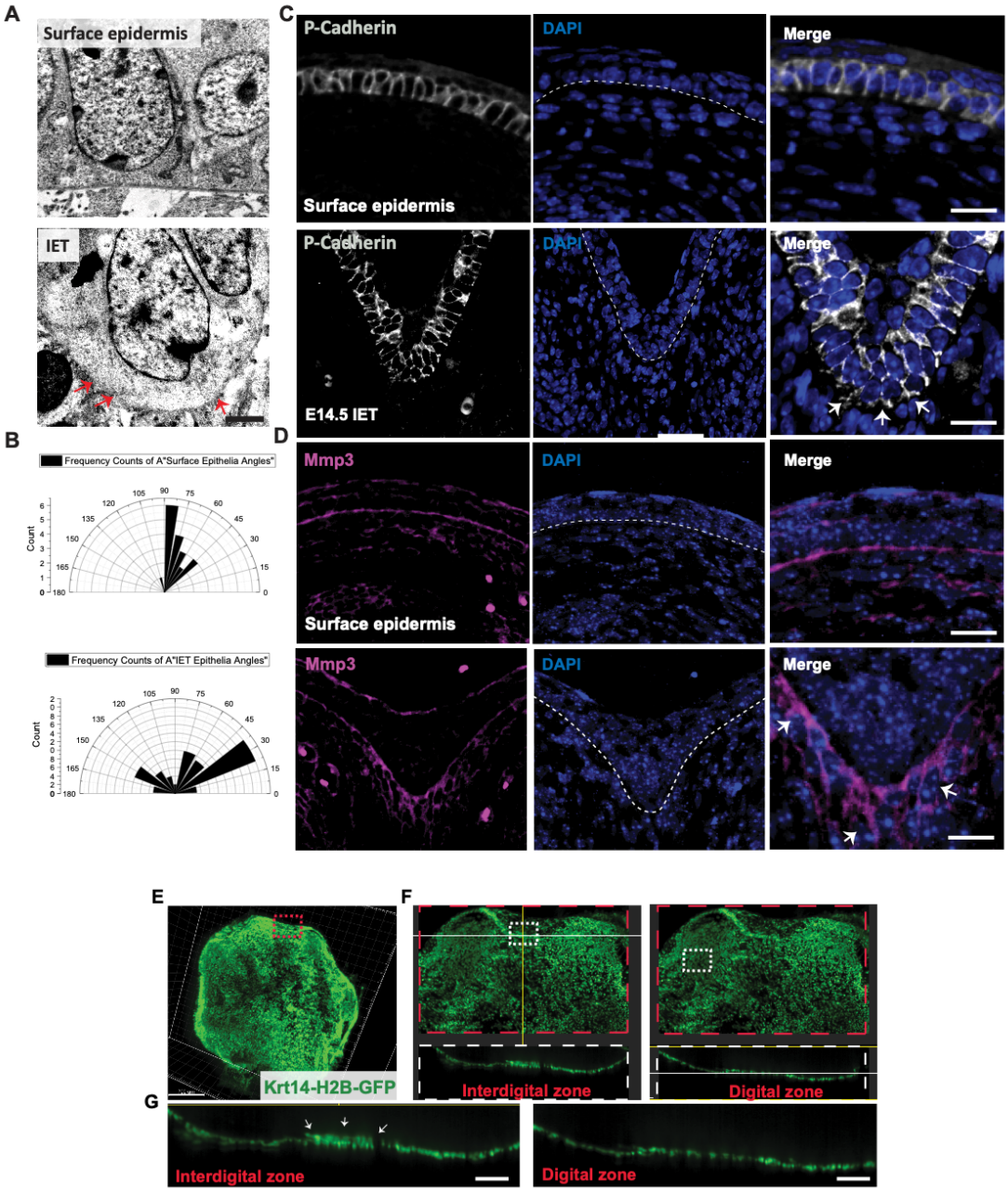

Figure S3. Related to Figure 5. Active cell migration of surface epidermal cells during digit separation
(A) EM images of a basal keratinocytes in the surface epidermis (left) and IET (right) (magnified portions of TEM images from main Figure 5A). Red arrows indicate cell protrusions. (B) Measurements of the orientation of the nucleus in basal keratinocytes located at the surface epidermis and IET relative to the basement membrane. (C) Immunofluorescence staining with the cell adhesion molecule P-Cadherin (gray) in surface epidermis and IET. Arrows indicate the apical expression of p-cadherin at the IET leader cells. Right panels show higher-magnification images. (D) Immunofluorescence staining with the extracellular matrix enzyme-matrix metalloproteinase-3 MMP3 (Magenta). Arrows indicate the cells with high expression of Mmp3. Right panels show higher-magnification images. (E) 3D stack of embryonic forelimb epithelia (Green) collected with light-sheet fluorescence microscopy. Red-dashed box

indicated the interdigital zone between digit 3 and 5. (F) Orthro-slice view of 3D stack at the interdigital zone (left) and a digital zone(right). (G) Higher magnification images of panel F. Arrows indicate the multilayered positive Krt14-H2B-GFP- cells in the interdigital zone.

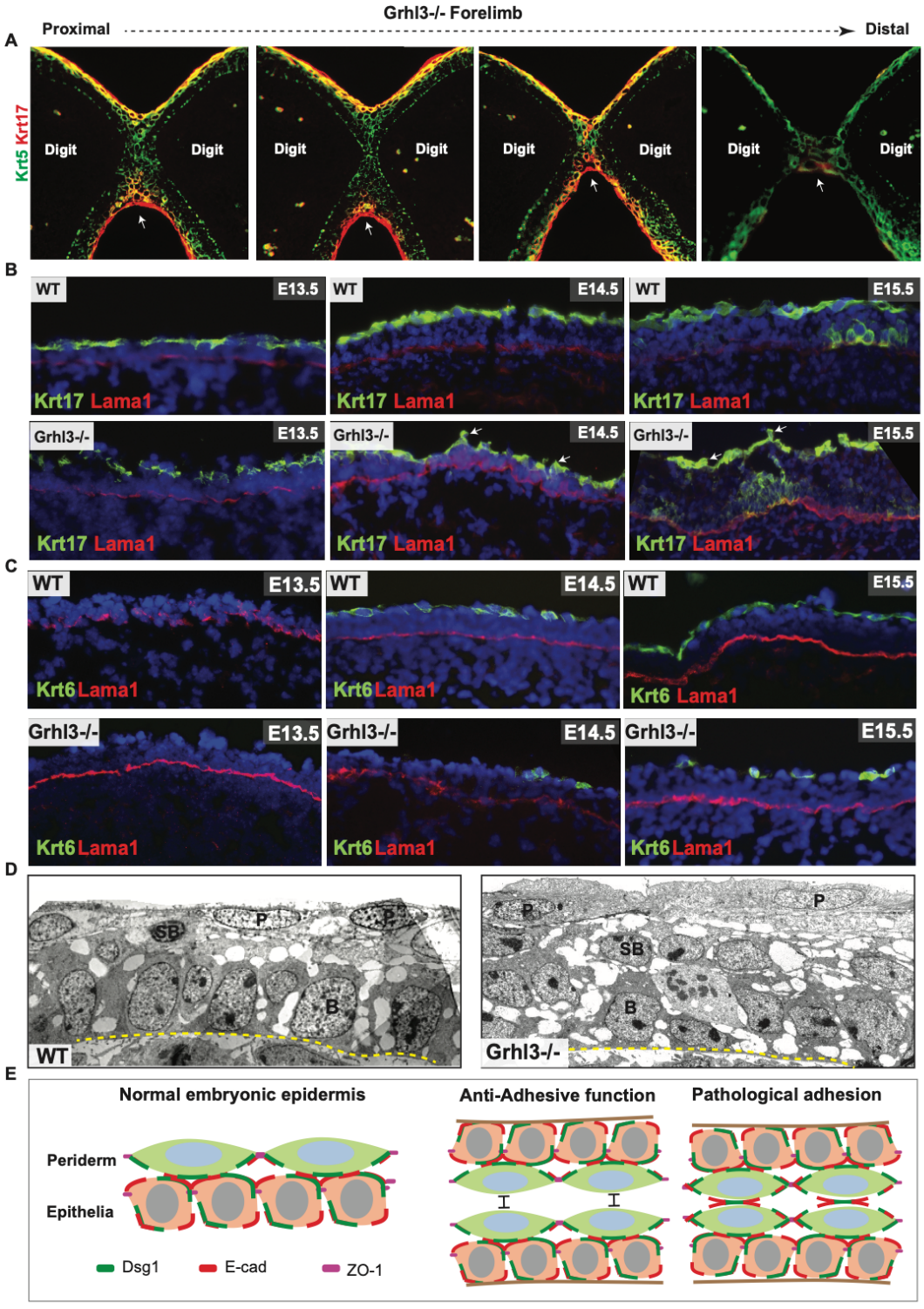

Figure S4. Related to Figure 6 and 7. GRHL3 is required for normal periderm formation and the non-adhesive function of periderm

(A) Series of images showing the interdigital epithelia stained with keratin-5 (green) and keratin-17 (red) in continuous ortho-slices of 3D reconstructions in *Grhl3*$^{-/-}$ forelimbs at E15.5. Arrows indicate the accumulation of

periderm cells in the interdigital zone. (B-C) Immunofluorescence staining of the early periderm marker keratin-17 (green), the late periderm marker Keratin-6 (green) and basement membrane marker Laminin 1 (Red) in embryonic skin sections collected from WT and *Grhl3*$^{-/-}$ embryos at E13.5, E14.5 and E15.5, respectively. White arrows indicate the spiky morphology of periderm cells. (D) Transmission Electron microscopy analysis of surface epithelia at E14.5 indicate abnormal periderm cells in *Grhl3*$^{-/-}$ epidermis compared to periderm cells in WT epidermis (P, periderm; SB, suprabasal keratinocytes; B, basal keratinocytes). Dashed-line outlines the basement membrane. (E) Schematic representation of the restricted expression of adhesion molecules in periderm cells and periderm cells non-adhesive function.

Table 1. Related to Figure 7. List of selected differentially expressed genes in *Grhl3*$^{-/-}$ forepaws at E14.5.

Genes	logFC	PValue
Rpl9-ps6	-15.60908423	0.00E+00
Krt8	2.988359342	1.37E-38
Klk7	6.267961843	5.17E-37
Cdsn	6.940888415	3.52E-33
Krt75	3.433560489	3.32E-29
Ifi202b	3.121897959	4.98E-28
Krt17	3.311217285	1.38E-26
Krt6a	3.907742757	3.45E-26
Krt9	2.938038292	1.54E-23
BC100530	3.970450924	1.68E-23
Nat8l	2.170635914	9.51E-23
Krt16	5.847486198	3.90E-22
Spink12	5.327475553	5.46E-22
Gm8162	8.137295717	1.66E-21
Rps2-ps6	2.813943438	9.54E-19
Krt79	6.236883647	2.35E-18
C130079G13Rik	-3.923381157	1.12E-17
Krt13	4.271710893	1.82E-17
Krt18	1.873178553	8.64E-16
Sprr2a1	3.118379683	3.71E-15
Plet1	3.325145927	1.30E-14
Urah	2.674560321	1.74E-14
Krt6b	6.915706944	2.77E-14
Gm9696	-3.4200521	8.75E-14
Gm10093	1.229635598	3.20E-13
Grhl3	-3.140189957	4.10E-13
Cldn6	1.6005674	4.32E-13
Gjb4	3.92673726	1.07E-12
Snx31	-3.254863755	1.87E-12
Atp6v1c2	6.947128681	3.96E-12
Krt84	2.19742052	4.03E-12
Hspb8	1.060454321	4.42E-12
Krt7	1.595518329	5.08E-12
Slc26a9	4.903278623	1.70E-11
F2rl1	1.592862258	2.25E-11
Cdkn1a	0.939768043	2.25E-05

Fhl2	1.17230373	2.33E-05
Slc9a2	-2.331467251	2.33E-05
Glb1l2	1.001554683	2.44E-05
Panx3	-1.390564392	2.45E-05
Anxa3	0.714545777	2.62E-05
Trnp1	-1.194569639	2.75E-05
Tmem254a	-1.25970287	2.78E-05
Aox4	-1.382808502	4.74E-05
Fzd6	0.71425225	4.84E-05
Col4a6	0.934938927	6.10E-05
Irf6	0.630048351	6.85E-05
Dsg3	2.109587411	7.57E-05
Serpinb2	1.82753079	7.70E-05
Wnt10a	0.740218655	7.85E-05
Gm6741	-1.463549534	7.94E-05
Myh11	0.955237956	8.29E-05
Creg2	1.158160507	8.92E-05
Bpifc	-1.497646301	9.19E-05
Hoxa11	-0.497464648	9.44E-05
Serpinb7	1.608066635	9.81E-05
Upk3b	-1.849116588	0.001048372
Vav3	0.597289962	0.001078682
Sfn	0.737573433	0.001082981
Zfp185	-0.549789976	0.001157852
Gprc5a	0.985405715	0.001193163
Cdh1	0.788709808	0.002176802
Hist1h1c	0.453761764	0.014504648
Il1f9	-0.782709295	0.014547902
Stxbp2	0.380759271	0.014567587
Ephb2	0.29927198	0.014582874
Tcirg1	-0.379507973	0.014662743
Slc2a4rg-ps	-0.549800497	0.024514522
Shisa3	-0.428693611	0.024568795
Ripk4	0.428366767	0.024670124
Nectin2	0.27312852	0.024787132
Plcd1	-0.301912044	0.02507265
Gpr20	0.711465465	0.025314858
Phf1	-0.303981712	0.025413379